Smart Mater. Struct. **10** (2001) 970–978 PII: S0964-1726(01)27541-7

Influence of applied electric field on the energy release rate for cracked PZT/elastic laminates

Xiaoxia Wu[1,2], **Jinquan Cheng**[1,3,4] **and Biao Wang**[1]

[1] Center for Composite Materials and Electro-optics Research Center, Harbin Institute of Technology, Harbin, 150001, People's Republic of China
[2] Department of Mechanical Engineering, Hong Kong University of Science and Technology, Clear Water Bay, Kowloon, Hong Kong
[3] Institute of High Performance Computing, 89-C Science Park Drive, #02-11/12 The Rutherford, Singapore Science Park 1, Singapore 118261

E-mail: chengjq@ihpc.nus.edu.sg

Received 29 January 2001, in final form 10 May 2001
Published 3 October 2001
Online at stacks.iop.org/SMS/10/970

Abstract
Since the delamination induced failure of a laminated smart structure always occurs under the action of mechanical and electrical fields, a generalized two-dimensional model for a piezoelectric/elastic laminate is established in order to analyze the effect of an applied electric field on its delamination. First, based on the double Fourier series method, a general analytical solution of the mid-plane displacement is derived for any boundary condition. Furthermore, the energy release rate is employed to study the influence of the applied electric field and mechanical loading on the fracture characteristics of the piezoelectric/elastic laminate. The energy release rates for modes I and II fracture behavior of the PZT/elastic laminates are calculated in detail. Such calculations indicate that it is feasible to choose not only suitable material properties of the piezoelectric and elastic layers, but also their thicknesses, to improve the smart structure's fracture strength within a specified range.

1. Introduction

Recently, smart materials, such as PZT, $BaTiO_3$ and PLZT etc, have been widely used in smart structures, for instance actuators, sensors etc [1–3]. Generally, the smart structures are composed of some smart material layers and elastic layers such as steel, composite etc. Since the devices are always subjected to combined strong electric fields and mechanical loading, debonding may occur at the interface between the smart material layers and the elastic layers [1, 4, 5]. The debonding can significantly alter not only the dynamic response, including the open- and closed-loop frequencies but also the control authority of the smart structure, and can even induce the smart structure's failure. Then, the reliability problem of these devices becomes one of the most predominant issues for the wider application of the smart materials and structures.

[4] Author to whom correspondence should be addressed.

In recent years many theoretical analyses have been performed to investigate the static and dynamic mechanical properties of piezoelectric/elastic composites on the basis of the beam model [6, 7], the classic laminate theory (CLT) [8–12], the first-order Mindlin-type analysis [13] and higher-order theory [14–16], etc. However, there were few works on studying the effect of external electric and mechanical field on the failure behavior of the piezoelectric/elastic laminate. Recently, some experimental and theoretical works were carried out by Seeley and Chattopadhyay [4, 5] and Cheng *et al* [17] in order to verify the effect of the electric field on smart structures' debonding.

In the present paper, we establish a generalized two-dimensional model for a cracked composite plate integrated with a piezoelectric layer and an elastic layer in order to study their delamination problem. Then on the basis of the developed double Fourier series, an analytical solution

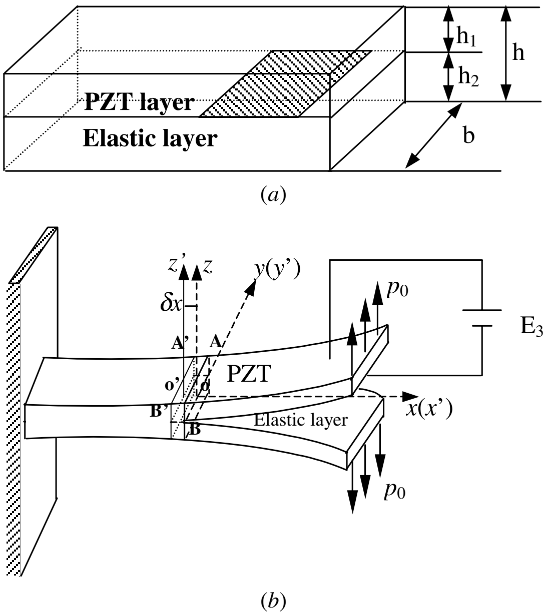

Figure 1. The generalized two-dimensional model shows a delamination inside the piezoelectric/elastic composite. (*a*) Deformation geometry (*b*) debonding extends to δa.

for the displacement of a smart plate for any boundary conditions is obtained. Furthermore, the energy release rate is derived in order to analyze the effect of the electric field on the delamination of the smart composite structures.

2. Generalized two-dimensional model for a delamination

In order to describe the delamination problem of the smart laminate, we consider a delamination in a composite plate, integrated with one upper piezoelectric layer with thickness h_1 and one lower elastic layer with the thickness h_2 as shown in figure 1. This is a thin sheet of thickness h and width b containing a delamination with the length a, or a crack in the interface between the piezoelectric layer and the elastic layer. It is assumed that the poling direction of piezoelectric layer is along the z-axis. It is no doubt that the delamination could either propagate or close under the action of the external mechanical load or electric field.

In order to obtain the elastic fields of each layer before and after the delamination extension δx along the x-direction, we employ the CLT to investigate the elastic fields of a plate. If the crack tip is taken to be originally at o and then move to o$'$ as shown in figure 1, we may take the original displacements and rotations of the laminate as $u_i^{00}(x_i)$ and $\phi_i^{00}(x_i)$ at o$'$ to $\phi_i^{00} + (\mathrm{d}\phi_i^{00}/\mathrm{d}x_j)\delta x_j$ and $u_i^{00} + (\mathrm{d}u_i^{00}/\mathrm{d}x_j)\delta x_j$ at o ($i, j = 1, 2$ and $x_1 = x$, $x_2 = y$). When the crack tip in the original point moves from o to o$'$, the displacements and rotations of the upper '1' and lower '2' lamina at o will be $(\mathrm{d}u_i^1/\mathrm{d}x_j)\delta x_j$, $(\mathrm{d}\phi_i^1/\mathrm{d}x_j)\delta x_j$ and $(\mathrm{d}u_i^2/\mathrm{d}x_j)\delta x_j$, $(\mathrm{d}\phi_i^2/\mathrm{d}x_j)\delta x_j$. In terms of the CLT and the relationships between the strains and displacements, the strains' change of the relevant lamina due to the crack extension δx can be determined as follows:

$$\left(\frac{\mathrm{d}u_i^1}{\mathrm{d}x_j} - \frac{\mathrm{d}u_i^{00}}{\mathrm{d}x_j}\right)\delta x_j \qquad \left(\frac{\mathrm{d}\phi_i^1}{\mathrm{d}x_j} - \frac{\mathrm{d}\phi_i^{00}}{\mathrm{d}x_j}\right)\delta x_j$$

$$\left(\frac{\mathrm{d}u_i^2}{\mathrm{d}x_j} - \frac{\mathrm{d}u_i^{00}}{\mathrm{d}x_j}\right)\delta x_j \qquad \text{and} \qquad \left(\frac{\mathrm{d}u_i^2}{\mathrm{d}x_j} - \frac{\mathrm{d}\phi_i^{00}}{\mathrm{d}x_j}\right)\delta x_j.$$

Therefore, extending Williams' [18] one-dimensional model for the crack laminates to the two-dimensional delamination problem, we can calculate the free energy change of the PZT/elastic laminate due to the delamination extension of a fictitious length δx, as shown in figure 1(b). After integrating the energy through the thickness h_1 and h_2 for each layer we can present the energy release rate for the delamination of the laminated plate as follows:

$$G = \frac{1}{2b}\left[\int_{\mathrm{PZT}} [N_\mathrm{p}(\varepsilon^1 - \varepsilon^{00}) + M_\mathrm{p}(-k^1 + k^{00})]\,\mathrm{d}x\,\mathrm{d}y + \int_{\mathrm{Ela}} [N_\mathrm{e}(\varepsilon^2 - \varepsilon^{00}) + M_\mathrm{e}(-k^2 + k^{00})]\,\mathrm{d}x\,\mathrm{d}y\right] \tag{1}$$

where $\varepsilon_{ij} = \mathrm{d}u_i/\mathrm{d}x_j$, $\phi_i = \mathrm{d}w/\mathrm{d}x_i$ and $-k_{ij} = \mathrm{d}\phi_i/\mathrm{d}x_j$ ($i, j = 1, 2$) are used. N_p, M_p, N_e and M_e are the forces and moments of the PZT lamina and the elastic lamina at o, respectively.

It is explicitly indicated that we must compute the strains ε and the rotations ϕ of the piezoelectric lamina and elastic lamina with the clamped edge AB, respectively. Therefore, we have to analyze a plate (piezoelectric plate and elastic plate) with the boundary conditions of one edge clamped and other edges free.

3. Analytic solution of the composite plates with integrated piezoelectric layer

Using the CLT to analyze the piezoelectric plate, we have the constitutive relationship of the piezoelectric lamina and elastic lamina in the following formation:

$$\begin{Bmatrix} \sigma_x \\ \sigma_y \\ \tau_{xy} \end{Bmatrix}_k = \begin{bmatrix} Q_{11} & Q_{12} & Q_{16} \\ Q_{12} & Q_{22} & Q_{26} \\ Q_{16} & Q_{26} & Q_{66} \end{bmatrix}_k \left[\begin{Bmatrix} \varepsilon_x \\ \varepsilon_y \\ \varepsilon_{xy} \end{Bmatrix}_k - \begin{Bmatrix} d_{31}E_3 \\ d_{31}E_3 \\ 0 \end{Bmatrix}_k\right] \tag{2}$$

where Q_{ij} are the stiffness tensors, d_{31} is the piezoelectric constant and E_3 is the applied external electric field along the poling direction (z-axis) of the piezoelectric layer. The subscript k denotes the kth layer of the laminated composite plate. For the elastic layer, the electric-induced strain, for example the second part of the right-hand side in equation (2), is equal to zero.

In the light of the Kirchhoff hypothesis, the strain of a plate may be written as the function of the mid-plane displacement u_0, v_0 and the transverse deflection w in the following form:

$$\varepsilon_x = \frac{\partial u_0}{\partial x} - z\frac{\partial^2 w}{\partial x^2}$$

$$\varepsilon_y = \frac{\partial v_0}{\partial y} - z\frac{\partial^2 w}{\partial y^2}$$

$$\gamma_{xy} = \left(\frac{\partial u_0}{\partial y} - \frac{\partial v_0}{\partial x}\right) - 2x\frac{\partial^2 w}{\partial x \partial y}. \tag{3}$$

Furthermore, the resultant forces and moments are defined by

$$\begin{Bmatrix} N_x \\ N_y \\ N_{xy} \end{Bmatrix} = \int_{-h/2}^{h/2} \begin{Bmatrix} \sigma_x \\ \sigma_y \\ \tau_{xy} \end{Bmatrix} \mathrm{d}z = \begin{bmatrix} A_{11} & A_{12} & A_{16} \\ A_{12} & A_{22} & A_{26} \\ A_{16} & A_{26} & A_{66} \end{bmatrix} \begin{Bmatrix} \varepsilon_x^0 \\ \varepsilon_y^0 \\ \varepsilon_{xy}^0 \end{Bmatrix} + \begin{bmatrix} B_{11} & B_{12} & B_{16} \\ B_{12} & B_{22} & B_{26} \\ B_{16} & B_{26} & B_{66} \end{bmatrix} \begin{Bmatrix} k_x \\ k_y \\ k_{xy} \end{Bmatrix} + \sum_{k=1}^{n} (z_k - z_{k-1}) \begin{Bmatrix} e_{31}E_3 \\ e_{31}E_3 \\ 0 \end{Bmatrix} \tag{4a}$$

$$\begin{Bmatrix} M_x \\ M_y \\ M_{xy} \end{Bmatrix} = \int_{-h/2}^{h/2} \begin{Bmatrix} \sigma_x \\ \sigma_y \\ \tau_{xy} \end{Bmatrix} z\,\mathrm{d}z = \begin{bmatrix} B_{11} & B_{12} & B_{16} \\ B_{12} & B_{22} & B_{26} \\ B_{16} & B_{26} & B_{66} \end{bmatrix} \begin{Bmatrix} \varepsilon_x^0 \\ \varepsilon_y^0 \\ \varepsilon_{xy}^0 \end{Bmatrix} + \begin{bmatrix} D_{11} & D_{12} & D_{16} \\ D_{12} & D_{22} & D_{26} \\ D_{16} & D_{26} & D_{66} \end{bmatrix} \begin{Bmatrix} k_x \\ k_y \\ k_{xy} \end{Bmatrix} + \sum_{k=1}^{n} \frac{1}{2}(z_k^2 - z_{k-1}^2) \begin{Bmatrix} e_{31}E_3 \\ e_{31}E_3 \\ 0 \end{Bmatrix} \tag{4b}$$

where the following definitions are used

$$\begin{Bmatrix} \varepsilon_x^0 \\ \varepsilon_y^0 \\ \varepsilon_{xy}^0 \end{Bmatrix} = \begin{Bmatrix} \dfrac{\partial u_0}{\partial x} \\ \dfrac{\partial v_0}{\partial y} \\ \dfrac{\partial u_0}{\partial y} + \dfrac{\partial v_0}{\partial x} \end{Bmatrix}$$

and

$$\begin{Bmatrix} k_x \\ k_y \\ k_{xy} \end{Bmatrix} = - \begin{Bmatrix} \dfrac{\partial^2 w}{\partial x^2} \\ \dfrac{\partial^2 w}{\partial y^2} \\ 2\dfrac{\partial^2 w}{\partial x \partial y} \end{Bmatrix} \tag{5}$$

the stiffness matrixes are calculated by

$$A_{ij} = \sum_{k=1}^{N} (Q_{ij})_k (z_k - z_{k-1})$$

$$B_{ij} = \frac{1}{2} \sum_{k=1}^{N} (Q_{ij})_k (z_k^2 - z_{k-1}^2)$$

$$D_{ij} = \frac{1}{3} \sum_{k=1}^{N} (Q_{ij})_k (z_k^3 - z_{k-1}^3)$$

and the piezoelectric constants are derived from

$$e_{kij} = Q_{ijmn} d_{kmn}.$$

Since the piezoelectric layer in some smart structures is required not to be completely covered by electrode in order to perform some functions, the effect of electrode needs to be taken into consideration. On the other hand, the strength of the polarization field can be changed or depoled if the lamina is made from the material with ferroelectric behavior such as PVDF, PZT etc. Therefore, d_{31} can be varied along the x–y plane. In order to consider the effect of polarization and electrodes, Lee [9] expressed the practical piezoelectric constant d_{31} by

$$d_{31} = d_{310} P(x, y)$$

where d_{310} is obtained from specifications or measurement. $P(x, y)$ is determined by the electrode pattern of the piezoelectric layer.

While the surface of piezoelectric plate are completely covered by the electrode, $P(x, y)$ can be presented by

$$P(x, y) = [H(x) - H(x - a)] \times [H(y) - H(y - b)]$$

where $H(x)$ is the Heaviside function, a and b are the length and width of the piezoelectric plate.

Furthermore, the equilibrium equations of a plate (elastic or piezoelectric) can be described by

$$\frac{\partial N_x}{\partial x} + \frac{\partial N_{xy}}{\partial y} = 0 \qquad \frac{\partial N_y}{\partial y} + \frac{\partial N_{xy}}{\partial x} = 0 \tag{6a}$$

$$\frac{\partial^2 M_x}{\partial x^2} + 2\frac{\partial^2 M_{xy}}{\partial x \partial y} + \frac{\partial^2 M_y}{\partial y^2} = p_0 \tag{6b}$$

and the relevant pre-described boundary conditions must be satisfied along the x- and y-axial edges as follows:

$$u_n = \overline{u}_n \quad \text{or} \quad N_n = \overline{N}_n$$

$$u_t = \overline{u}_t \quad \text{or} \quad N_{nt} = \overline{N}_{nt}$$

$$w_{,n} = \overline{w}_{,n} \quad \text{or} \quad M_n = \overline{M}_n$$

$$w = \overline{w} \quad \text{or} \quad M_{nt,t} + Q_n = \overline{K}_n.$$

Substituting equation (5) into equation (6) can yield

$$\begin{aligned} & A_{11}\frac{\partial^2 u_0}{\partial x^2} + A_{66}\frac{\partial^2 u_0}{\partial y^2} + 2A_{16}\frac{\partial^2 u_0}{\partial x \partial y} + A_{16}\frac{\partial^2 v_0}{\partial x^2} \\ & \quad + (A_{12} + A_{66})\frac{\partial^2 v_0}{\partial x \partial y} + A_{26}\frac{\partial^2 v_0}{\partial y^2} - B_{11}\frac{\partial^3 w}{\partial x^3} \\ & \quad - 3B_{16}\frac{\partial w^3}{\partial x^2 \partial y} - (B_{12} + 2B_{66})\frac{\partial w^3}{\partial x \partial y^2} - B_{26}\frac{\partial w^3}{\partial y^3} \\ & = \sum_{k=1}^{n} (z_k - z_{k-1}) e_{31} E_3 \\ & \quad \times \frac{\partial \{[H(x) - H(x - a)] \times [H(y) - H(y - b)]\}}{\partial x} \end{aligned}$$

$$\begin{aligned} & A_{16}\frac{\partial^2 u_0}{\partial x^2} + A_{26}\frac{\partial^2 u_0}{\partial y^2} + (A_{12} + A_{66})\frac{\partial^2 u_0}{\partial x \partial y} + A_{66}\frac{\partial^2 v_0}{\partial x^2} \\ & \quad + 2A_{26}\frac{\partial^2 v_0}{\partial x \partial y} + A_{22}\frac{\partial^2 v_0}{\partial y^2} - B_{16}\frac{\partial^3 w}{\partial x^3} - 3B_{26}\frac{\partial^3 w}{\partial x \partial y^2} \\ & \quad - (B_{12} + 2B_{66})\frac{\partial w^3}{\partial x^2 \partial y} - B_{22}\frac{\partial^3 w}{\partial y^3} \\ & = \sum_{k=1}^{n} (z_k - z_{k-1}) e_{31} E_3 \\ & \quad \times \frac{\partial \{[H(x) - H(x - a)] \times [H(y) - H(y - b)]\}}{\partial y} \end{aligned}$$

$$D_{11}\frac{\partial^4 w}{\partial x^4}+4D_{16}\frac{\partial^4 w}{\partial x^3\partial y}+2(D_{12}+2D_{66})\frac{\partial^4 w}{\partial x^2\partial y^2}$$
$$+4D_{26}\frac{\partial^4 w}{\partial x\partial y^3}+D_{22}\frac{\partial^4 w}{\partial y^4}-B_{11}\frac{\partial^3 u_0}{\partial y^3}-3B_{16}\frac{\partial^3 u_0}{\partial x^2\partial y}$$
$$-(B_{12}+2B_{66})\frac{\partial^3 u_0}{\partial x\partial y^2}-B_{26}\frac{\partial^3 u_0}{\partial y^3}-B_{16}\frac{\partial^3 v_0}{\partial x^3}$$
$$-(B_{12}+2B_{66})\frac{\partial^3 v_0}{\partial x\partial y^2}-3B_{26}\frac{\partial^3 v_0}{\partial x\partial y^2}-B_{22}\frac{\partial^3 v_0}{\partial y^3}=p_0. \tag{7}$$

It is clear that the equation (7) is a series of highly-coupled partial differential equations (PDEs) including the three-order and fourth-order partial differentials for the mid-plane displacements u_0, v_0 and w. In order to solve the highly-coupled equations (PDEs) with constant coefficients, a double Fourier series approach is employed to give the analytical solutions in the cases of the different boundary conditions, as indicated by Chaudhuri and Kabir [19–21]. This method facilitates the well-posedness of the Fourier analysis through selecting the coefficients of the assumed double Fourier series solutions for the unknown functions and introducing the certain boundary-discontinuous Fourier coefficients. After substituting those Fourier series solutions and their derivations into the equilibrium equations and the relevant boundary conditions, we can furnish a complete system of linear algebraic equations to derive the solutions, i.e. the number of equations is equal to the number of the unknown coefficients.

In terms of the equilibrium equation (7) and the pre-described boundary conditions of one edge clamped and three edges free, it is generally impossible to seek for a Fourier series solution suitable for both equilibrium conditions and boundary conditions simultaneously. Based on the developed double Fourier series approach, we can assume the following Fourier series solutions to reduce the equilibrium equations into a brief formula but not necessarily satisfy the pre-described condition:

$$u_0=\sum_{m=0}^{\infty}\sum_{n=1}^{\infty}U_{mn}\cos(\alpha_m x)\sin(\beta_n y)\qquad 0\leqslant x\leqslant a,\ 0<y<b$$
$$v_0=\sum_{m=1}^{\infty}\sum_{n=0}^{\infty}V_{mn}\sin(\alpha_m x)\cos(\beta_n y)\qquad 0<x<a,\ 0\leqslant y\leqslant b$$
$$w=\sum_{m=0}^{\infty}\sum_{n=1}^{\infty}W_{mn}\cos(\alpha_m x)\sin(\beta_n y)\qquad 0\leqslant x\leqslant a,\ 0<y<b \tag{8}$$

where $\alpha_m = m\pi/a$, $\beta_n = n\pi/b$ and a is the length of the delamination. However, we can introduce some unknown constant coefficients to satisfy the pre-described boundary conditions. It is clear that a system of the simplest linear algebraic equations can be easily derived through directly equating the coefficients of $\cos(\alpha_m x)\sin(\beta_n y)$, $\sin(\alpha_m x)\cos(\beta_n y)$ etc when the assumed Fourier series solutions and their derivatives obtained by the methods developed are substituted into the equilibrium equations. Thus, the work of computation can be reduced in a sense, which is the principle of the Fourier series solution's choice.

Since the boundary conditions along the edges $x = 0$ and $x = a$ are continuous, we have $u_0(0-0, y) = u_0(0+0, y)$ and $u_0(a-0, y) = u_0(-a+0, y)$. Therefore, $\partial u_0/\partial x$ can be obtained by term-wise differentiation as

$$\frac{\partial u_0}{\partial x}=\sum_{m=1}^{\infty}\sum_{n=1}^{\infty}-\alpha_m U_{mn}\sin(\alpha_m x)\sin(\beta_n y)\qquad 0<x<a,\ 0<y<b. \tag{9a}$$

However, since the boundary conditions along the edges $y = 0$ and $y = b$ are discontinuous, we can use the part integration to derive $\partial u_0/\partial y$ through introducing certain boundary-discontinuous Fourier coefficients as follows:

$$\frac{\partial u_0}{\partial y}=\frac{au_0}{4}+\frac{1}{2}\sum_{m=1}^{\infty}au_m\cos(\alpha_m x)+\frac{1}{2}\sum_{n=1}^{\infty}[\beta_n U_{0n}+\gamma_n au_0+\varphi_n bu_0]\cos(\beta_n y)+\sum_{m=1}^{\infty}\sum_{n=1}^{\infty}[\beta_n U_{mn}+\gamma_n au_m+\varphi_n bu_m]\cos(\alpha_m x)\cos(\beta_n y) \tag{9b}$$

where

$$(\gamma_m,\varphi_m)=\begin{cases}(0,1) & \text{if } m \text{ is odd}\\ (1,0) & \text{if } m \text{ is even}\end{cases}$$

and the following boundary-discontinuous Fourier coefficients are introduced:

$$(au_m, bu_m)=\frac{4}{ab}\int_0^a[\pm u_0(x,b)-u_0(x,0)]\cos(\alpha_m)\,\mathrm{d}x.$$

Heuristically in terms of the introduced constant coefficients, the discontinuous displacement functions and their derivatives at the boundaries may be obtained, for example as

$$u_0(x,b)=\sum_{m=0}^{\infty}\frac{b}{4}(au_m-bu_m)\cos(\alpha_m x) \tag{9c}$$

$$u_0(x,0)=\sum_{m=0}^{\infty}\frac{b}{4}(-au_m-bu_m)\cos(\alpha_m x). \tag{9d}$$

Extension of the above method to the second derivatives is straightforward, for example

$$\frac{\partial^2 u_0}{\partial x^2}=\frac{1}{2}\sum_{n=1}^{\infty}cu_n\sin(\beta_n y)+\sum_{m=1}^{\infty}\sum_{n=1}^{\infty}[-\alpha_m^2 U_{mn}+\gamma_m cu_n+\varphi_m du_n]+\cos(\alpha_m x)\sin(\beta_n y) \tag{10}$$

where the constant coefficients cu_n and du_n are introduced due to $\partial u_0/\partial x$ is discontinuous along the edges $x = 0$ and $x = a$, as presented in the appendix. Derivatives of other functions (v_0, w) can be obtained in a manner similar to the solution procedure for the derivatives of u_0 with respect to x and y. Expansion of the right-hand part (e.g. the external mechanical or electrical loading) of equation (7) into a double Fourier series and the substitution of the assumed functions and their derivatives into the left-hand part of equation (7), we obtain a system of linear algebraic equations through equating the coefficients of $\cos(\alpha_m x)\sin(\beta_n y)$, $\sin(\alpha_m x)\cos(\beta_n y)$ etc. In order to furnish a complete solution of the introduced constant coefficients, we must further substitute the assumed functions and their derivatives into the corresponding pre-described boundary conditions.

In the light of the generalized two-dimensional model, it is noted that we only need to solve the strains and stresses for the PZT lamina and the elastic lamina respectively. Therefore for the general commercial piezoelectric ceramic lamina, we have the stiffness matrixes $B_{ij} = 0$ and $A_{16} = A_{26} = 0$ in terms of the Kirchhoff hypothesis. For brevity, the solution procedure is illustrated only for the equilibrium equations (7*a*) and (7*b*) and the related boundary conditions. After the assumed Fourier series solutions and their derivatives are substituted into those equations, a system of $(2mn + 5n + 5m + 4)$ linear algebraic equations is obtained by equating the coefficients of $\cos(\alpha_m x)\sin(\beta_n y)$, $\sin(\alpha_m x)\cos(\beta_n y)$, $\sin(\alpha_m x)$, $\cos(\beta_n y)$ etc in the following formula.

The linear algebraic equations are obtained from the first and second expressions of equilibrium equation (7) as follows:

$$\begin{aligned}&A_{11}(\gamma_m cu_n + \varphi_m du_n - \alpha_m^2 U_{mn})\\&\quad -A_{66}\beta_n(\gamma_n au_m + \varphi_n bu_m + \beta_n U_{mn}) - (A_{12} + A_{66})\beta_n\\&\quad \times(\gamma_m av_n + \varphi_m bv_n + \alpha_m V_{mn})\\&\quad = \frac{4e_{31}E_3(1-(-1)^m)(1-(-1)^n)}{ab\beta_n}\end{aligned} \tag{11a}$$

$$\begin{aligned}&-\frac{1}{2}A_{66}au_0\gamma_n\beta_n - \frac{1}{2}A_{12}av_n\beta_n - \frac{1}{2}A_{66}av_n\beta_n\\&\quad -\frac{1}{2}A_{66}bu_0\varphi_n\beta_n + \frac{1}{2}A_{11}cu_n - \frac{1}{2}A_{66}\beta_n^2 U_{0n}\\&\quad = \frac{4e_{31}E_3(1-(-1)^n)}{ab\beta_n}\end{aligned} \tag{11b}$$

$$\begin{aligned}&-(A_{12} + A_{66})\alpha_m(\gamma_n au_m + \varphi_n bu_m + \beta_n U_{mn})\\&\quad -A_{66}\alpha_m(\gamma_m av_n + \varphi_m bv_n + \alpha_m V_{mn})\\&\quad +A_{22}(\gamma_n cv_m + \varphi_n dv_m - \beta_n^2 V_{mn})\\&\quad = \frac{4e_{31}E_3(1-(-1)^m)(1-(-1)^n)}{ab\alpha_m}\end{aligned} \tag{11c}$$

$$\begin{aligned}&-\frac{1}{2}A_{66}av_0\gamma_m\alpha_m - \frac{1}{2}A_{12}au_m\alpha_m - \frac{1}{2}A_{66}au_m\alpha_m\\&\quad -\frac{1}{2}A_{66}bv_0\varphi_m\alpha_m + \frac{1}{2}A_2 cv_m - \frac{1}{2}A_{66}\alpha_m^2 V_{0m}\\&\quad = \frac{4e_{31}E_3(1-(-1)^m)}{ab\alpha_n}.\end{aligned} \tag{11d}$$

From the boundary conditions of one edge clamped and other edges free, the other linear algebraic equations can be obtained; for example in terms of the boundary condition $u(0, y) = 0$, substituting $x = 0$ into the assumed double Fourier series solution of u and equating the coefficient of $\sin(\beta_n y)$ to zero yields

$$U_{0n} + \sum_{m=1}^{\infty} U_{mn} = 0. \tag{11e}$$

From the boundary condition $v(0, y) = 0$ and the introduced boundary-discontinuous Fourier series coefficients of v, i.e. equation (A3) shown in the appendix, equating the coefficients of $\cos(\beta_n y)$ to zero yields

$$av_0 + bv_0 = 0 \tag{11f}$$

$$av_n + bv_n = 0. \tag{11g}$$

In the same manner, we can obtain other linear algebraic equations from the other boundary conditions as follows:

$$\begin{aligned}&Q_{11}\frac{a}{4}(cu_n - du_n) - Q_{12}\beta_n\frac{a}{4}(av_n - bv_n)\\&\quad = \frac{e_{31}E_3(1-(-1)^n)}{b\beta_n}\end{aligned} \tag{11h}$$

$$\begin{aligned}&\frac{au_0}{4} + \sum_{m=1}^{\infty}\frac{1}{2}au_m(-1)^m + \frac{av_0}{4}\\&\quad + \sum_{m=\infty}^{\infty}\frac{1}{2}(av_0\gamma_m + bv_0\varphi_m + \alpha_m V_{0m})(-1)^m = 0\end{aligned} \tag{11i}$$

$$\begin{aligned}&\sum_{m=1}^{\infty}(\gamma_n au_m + \varphi_n bu_m + \beta_n U_{mn})(-1)^m\\&\quad +\frac{1}{2}(au_0\gamma_n + bu_0\varphi_n + \beta_n U_{0n}) + \frac{1}{2}av_n\\&\quad + \sum_{m=1}^{\infty}(\gamma_m av_n + \varphi_m bv_n + \alpha_m V_{mn})(-1)^m = 0\end{aligned} \tag{11j}$$

$$\begin{aligned}&\frac{au_0}{4} + \sum_{n=1}^{\infty}\frac{1}{2}(au_0\gamma_n + bv_0\varphi_n + \beta_n U_{0n}) + \frac{av_0}{4}\\&\quad + \sum_{n=1}^{\infty}\frac{1}{2}av_n = 0\end{aligned} \tag{11k}$$

$$\begin{aligned}&\sum_{n=1}^{\infty}(\gamma_n au_m + \varphi_n bu_m + \beta_n U_{mn}) + \frac{1}{2}au_m\\&\quad +\frac{1}{2}(av_0\gamma_m + bv_0\varphi_m + \alpha_m V_{0m})\\&\quad + \sum_{n=1}^{\infty}(\gamma_m av_n + \varphi_m bv_n + \alpha_m V_{mn}) = 0\end{aligned} \tag{11l}$$

$$\begin{aligned}&\frac{au_0}{4} + \sum_{n=1}^{\infty}\frac{1}{2}(au_0\gamma_n + bv_0\varphi_n + \beta_n U_{0n})(-1)^n + \frac{av_0}{4}\\&\quad + \sum_{n=1}^{\infty}\frac{1}{2}av_n(-1)^n = 0\end{aligned} \tag{11m}$$

$$\begin{aligned}&\sum_{n=1}^{\infty}(\gamma_n au_m + \varphi_n bu_m + \beta_n U_{mn})(-1)^n + \frac{1}{2}au_m\\&\quad +\frac{1}{2}(av_0\gamma_m + bv_0\varphi_m + \alpha_m V_{0m})\\&\quad + \sum_{n=1}^{\infty}(\gamma_m av_n + \varphi_m bv_n + \alpha_m V_{mn})(-1)^n = 0\end{aligned} \tag{11n}$$

$$\begin{aligned}&-Q_{22}\frac{b}{4}(cv_m + dv_m) + Q_{21}\alpha_m\frac{b}{4}(au_m + bu_m)\\&\quad = \frac{e_{31}E_3(1-(-1)^m)}{a\alpha_m}\end{aligned} \tag{11o}$$

$$\begin{aligned}&Q_{22}\frac{b}{4}(cv_m - dv_m) - Q_{21}\alpha_m\frac{b}{4}(au_m - bu_m)\\&\quad = \frac{e_{31}E_3(1-(-1)^m)}{a\alpha_m}\end{aligned} \tag{11p}$$

where the unknown coefficients introduced are shown in detail in the appendix. The discontinuous displacement functions and their derivatives at the boundaries are presented by those introduced unknown coefficients, as well as equations (9*c*) and (9*d*) and the following differential and integral are used:

$$\frac{\partial H(x-x_0)}{\partial x} = \delta(x-x_0)$$

and

$$\int f(x)\delta(x-x_0) = f(x_0).$$

Furthermore, we can solve the complete linear algebraic equations so as to obtain all the constant coefficients introduced by the boundary discontinuity or differential induced discontinuity. Substituting these solutions into equation (5), we can easily obtain the mid-plane strains and curvatures of the piezoelectric layer at o. Thus, we can obtain the relevant forces and moments of the piezoelectric layer in terms of equation (4). In a similar manner, we can also obtain the curvatures and moments of the elastic plate with one edge clamped and others edges free. While the stress resultants and moment resultants of the upper '1' and lower '2' lamina are obtained, the stress resultants and moment resultants of the uncracked zone of the PZT/elastic laminate can be derived through balancing the forces and moments of the representative volume element (RVE), as shown in figure 1(b), as follows:

$$N_x^0 \qquad N_y^0 \qquad N_{xy}^0 \qquad M_x^0 \qquad M_y^0 \qquad M_{xy}^0.$$

Substituting the relevant stress resultants and moment resultants N_x^0, N_y^0, N_{xy}^0, M_x^0, M_y^0 and M_{xy}^0 into equation (4) yields the strains ε^{00} and curvatures k^{00} of the uncracked zone of the PZT/elastic laminated composite as

$$\begin{Bmatrix} \varepsilon^{00} \\ k^{00} \end{Bmatrix} = \begin{bmatrix} [B^{-1}A - D^{-1}B]^{-1}B^{-1} & -[B^{-1}A - D^{-1}B]^{-1}D^{-1} \\ [A^{-1}B - B^{-1}D]^{-1}A^{-1} & -[A^{-1}B - B^{-1}D]^{-1}B^{-1} \end{bmatrix} \begin{Bmatrix} N^0 \\ M^0 \end{Bmatrix}$$

where A, B and D are the stiffness matrixes of the PZT/elastic composite.

Furthermore, substituting the results of the strains and curvatures ε^{00}, k^{00}, ε^1, k^1, ε^2, k^2 and the stress resultants and moment resultants N_p, M_p, N_e, M_e into equation (1), we can obtain the energy release rate for the delamination extension in detail.

4. Simulations and discussions

In the present paper we are concerned with the calculation of the energy release rate but not the critical fracture energy release rate. According to the proposed two-dimensional fracture model for the composite plate integrated with a piezoelectric layer, the effect of the applied electric field on the energy release rate of a PZT/elastic composite plate of size $0.03 \times 0.007 \times 0.002$ m^3 is analyzed in detail. The material constants of the elastic layer and the PZT layer are presented as the following.

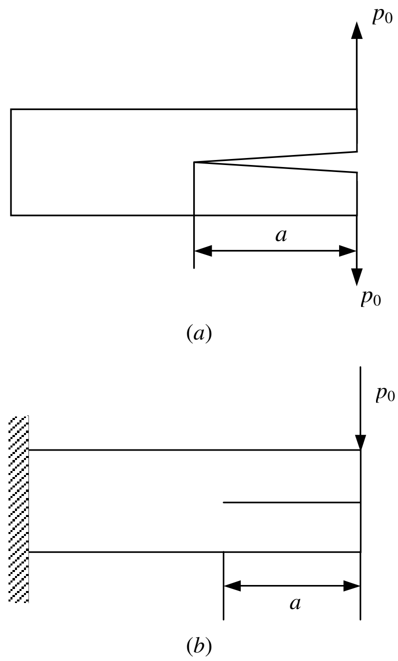

Figure 2. A common double cantilever beam experiment: (*a*) mode I fracture and (*B*) mode II fracture.

- Anisotropic elastic material I: Poisson's ratio $\nu_{12} = \nu_{33} = \nu_{23} = 0.3$, elastic modulus $E_{11} = 150$ GPa, $E_{22} = E_{33} = 9$ GPa, $G_{12} = G_{13} = 7.1$ GPa, $G_{23} = 2.5$ GPa.
- Isotropic elastic material II: Poisson's ratio $\nu_{12} = \nu_{33} = \nu_{23} = 0.3$, elastic modulus $E_{11} = E_{22} = E_{33} = 150$ GPa.
- PZT layer: Poisson ratio $\nu_{12} = \nu_{33} = \nu_{23} = 0.3$, piezoelectric constants $d_{31} = d_{32} = 254 \times 10^{-12}$ m V^{-1}, elastic modulus $E_{11} = 63$ GPa, $E_{22} = E_{33} = 63$ GPa, $G_{12} = G_{13} = 24.2$ GPa, $G_{23} = 24.2$ GPa.

In accordance with the detailed solution procedure for a PZT plate in section 3, we can obtain the strain, curvature, stress resultants and moments of the piezoelectric layer, elastic layer and an uncracking composite respectively. Then, the energy release rate is calculated in the cases of modes I and II fracture of a composite plate integrated with a PZT layer tested by a double cantilever beam test, as shown in figure 2.

For mode I fracture of PZT/material I and PZT/material II composite laminates, the simulations of the energy release rate are shown in figure 3 as a function of the applied electric field and the thickness ratio h_1/h_2 of the piezoelectric layer and elastic layer for a specified mechanical loading. Obviously, the correlation of the energy release rate and the applied electric field is shown as a parabolic curve with a symmetric axis about $E_3 \approx 0$ for both PZT/material I and PZT/material II composites. From figure 3(*a*), it is clear that both the positive and negative applied electric fields can advance the delamination inside PZT/material II extension in any case. However, for the PZT/material I composite, while the thickness ratio h_1/h_2 of the piezoelectric layer and elastic material I layer reaches a certain critical ratio ($h_1/h_2 = 9$) as indicated in figure 3(*b*), the energy release rate always decreases with increasing either the positive or

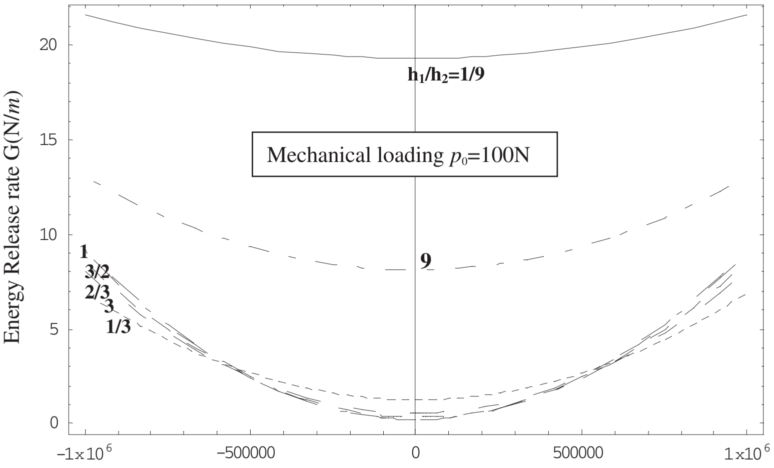

(*a*)

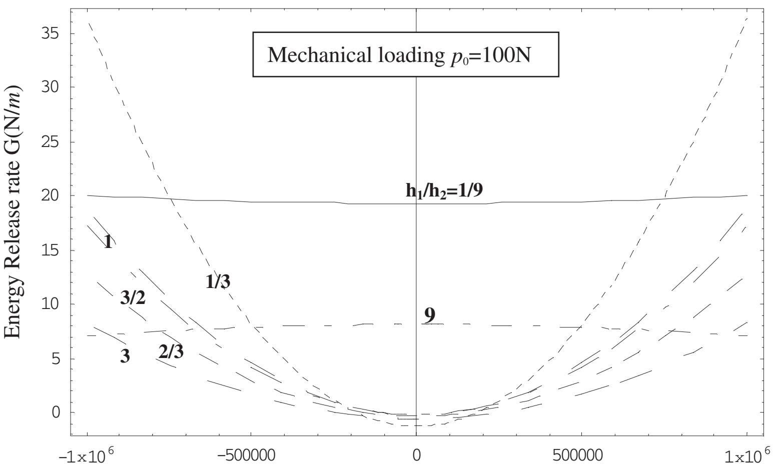

(*b*)

Figure 3. The influence of the applied electric field and the thickness ratio h_1/h_2 on the energy release rate for model I fracture for two of PZT/elastic composites: (*a*) PZT/isotropic material II composite and (*b*) PZT/anisotropic material I composite.

negative applied electric fields. This prediction indicates that both the positive and negative applied electric fields can prevent the delamination from extending. With regard to the effect of the thickness of the piezoelectric layer, the simulations indicate that the extreme values of the thickness ratio h_1/h_2 of the piezoelectric layer and elastic material II layer have a more predominant effect on the energy release rate than other values of the ratio, as depicted in figure 3(*a*). However, for PZT/material I composite laminate, the thickness effect on the energy release rate becomes less on increasing the external electric field.

For mode II fracture of PZT/material I and PZT/material II composites, the calculation of the energy release rate is depicted in figure 4 as a function of the applied electric field and the thickness ratio h_1/h_2 for a given mechanical loading p_0. The calculations indicate that the relationship between the energy release rate and the applied electric field also appears as a parabolic curve with a symmetric axis $E_3 = 73.98p_0$ for material I and $E_3 = 375.87p_0$ for material II. From figure 4(*a*), it is evident that both the negative and positive applied electric fields, excluding the range [0, $751.74p_0$], can promote the delamination propagation for the PZT/material II composite for any case. In contrast, the applied positive electric field in the range [0, $751.74p_0$] can enhance the fracture strength, which agrees with experimental results [17]. For the PZT/material I composite, both the negative and positive applied electric fields, excluding the range [0, $147.96p_0$], can improve the energy release rate when the thickness ratio h_1/h_2 is less than a certain critical value, as shown in figure 4(*b*). In comparison with the effect of the thickness of piezoelectric layer on the energy release rate in mode I fracture, either larger or smaller thickness ratios of the piezoelectric layer and elastic layer have less effect on the energy release rate for mode II fracture.

Meanwhile, the effect of the applied electric field and mechanical loading on the energy release rate for mode II fracture of the PZT/material II composite is shown in figure 5. The results also show that the energy release rate may decrease on increasing the applied electric field or mechanical loading.

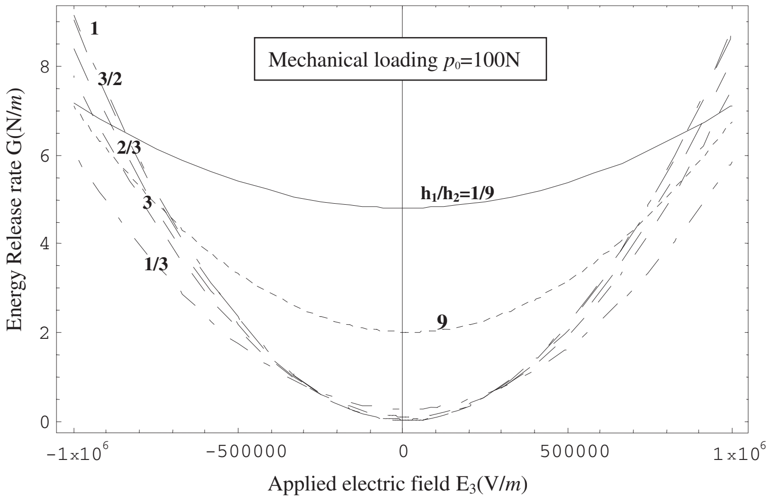

(*a*)

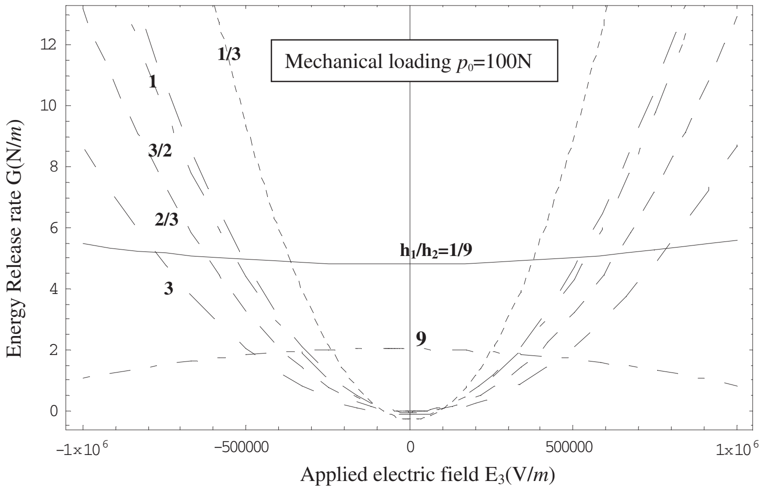

(*b*)

Figure 4. The influence of the applied electric field and the thickness ratio h_1/h_2 on the energy release rate for model II fracture of two PZT/elastic composites: (*a*) PZT/isotropic material II composite and (*b*) PZT/anisotropic material I composite.

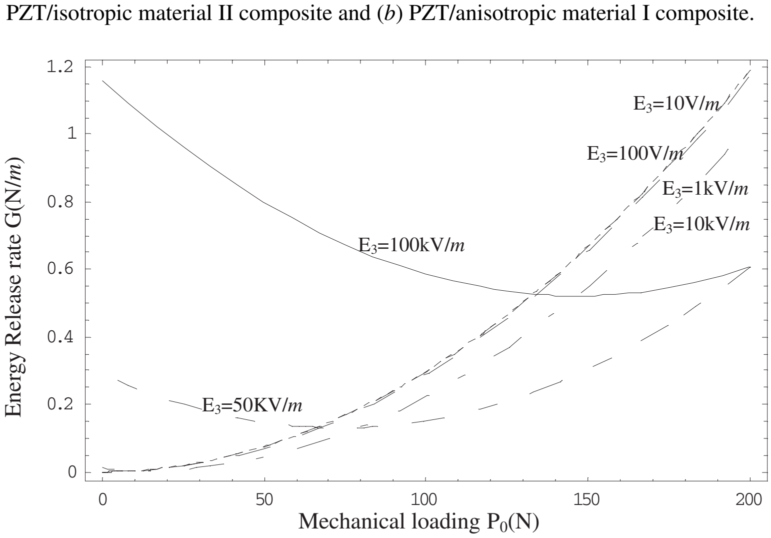

Figure 5. The effect of the applied external mechanical and electrical loading on the energy release rate for mode II fracture of a PZT/isotropic material composite.

In other words, the applied positive electric field can enhance the fracture strength in some cases.

In terms of the above calculations and discussion, it is shown that we can design optimal smart structures, such as specially required mechanical properties and reliability etc, by a method of selecting a suitable piezoelectric material and elastic material and their thickness ratio.

5. Conclusions

A generalized two-dimensional delamination model is established to investigate the effect of the applied electric field on the energy release rate of the delamination of piezoelectric/elastic laminates. The simulations for modes I and II fracture of the PZT/elastic laminates reveal that the effect of the positive and negative electric fields on the energy release rate of a smart structure is determined by the material properties of the smart layer and the elastic layer and their thickness ratio. Therefore, we can select the right material properties of each lamina in order to improve the fracture strength of smart structures.

Acknowledgment

The work was supported by the National Science Foundation of China with the Excellent Young Investigator Award.

Appendix

The boundary-discontinuous induced–introduced unknown constant coefficients are presented as follows

$$(au_m, bu_m) = \frac{4}{ab}\int_0^a [\pm u_0(x,b) - u_0(x,0)]\cos(\alpha_m x)\,\mathrm{d}x \tag{A1}$$

$$(cu_n, du_n) = \frac{4}{ab}\int_0^b [\pm u_{0,1}(a,y) - u_{0,1}(0,y)]\sin(\beta_n y)\,\mathrm{d}y \tag{A2}$$

$$(av_n, bv_n) = \frac{4}{ab}\int_0^b [\pm v_0(a,y) - v_0(0,y)]\cos(\beta_n y)\,\mathrm{d}y \tag{A3}$$

$$(cv_m, dv_m) = \frac{4}{ab}\int_0^a [\pm v_{0,2}(x,b) - v_{0,2}(x,0)]\sin(\alpha_m x)\,\mathrm{d}x \tag{A4}$$

$$(ew_n, fw_n) = \frac{4}{ab}\int_0^b [\pm w_{,12}(a,y) - w_{,12}(0,y)]\sin(\beta_n y)\,\mathrm{d}y \tag{A5}$$

$$(gw_m, hw_m) = \frac{4}{ab}\int_0^a [\pm w_{,22}(x,b) - w_{,22}(x,0)] + \cos(\alpha_m x)\,\mathrm{d}x \tag{A6}$$

$$(kw_n, lw_n) = \frac{4}{ab}\int_0^b [\pm w_{,111}(a,y) - w_{,111}(0,y)] + \sin(\beta_n y)\,\mathrm{d}y \tag{A7}$$

where the subscript $,i$ denotes the partial derivation for the mid-plane displacement u_0, v_0 and w with respect to the i-axis.

References

[1] Uchino K 1998 Piezoelectric ultrasonic motors: overview *Smart Mater. Struct.* **7** 273–85

[2] Haertling G H 1994 Rainbow ceramics—a new type of ultra-high-displacement actuator *Am. Ceram. Soc. Bull.* **73** 93–6

[3] Lee S-W Ricky and Li H L 1998 Development and characterization of a rotary motor driven by anisotropic piezoelectric composite laminate *Smart Mater. Struct.* **7** 327–36

[4] Seeley C E and Chattopadhyay A 1998 Experimental investigation of composite beams with piezoelectric beams with piezoelectric actuation and debonding *Smart Mater. Struct.* **7** 502–11

[5] Seeley C E and Chattopadhyay A 1999 Modeling of smart composite laminates including debonding: a finite element approach *Int J. Solids Struct.* **36** 1823–43

[6] Zhang X D and Sun C T 1996 Formulation of an adaptive sandwich beam *Smart Mater. Struct.* **5** 814–23

[7] Donthireddy P and Chandrasha K 1996 Modeling and shape control of composite beams with embedded piezoelectric actuators *Composite Struct.* **35** 237–44

[8] Crawley E and Anderson E 1989 Detailed model of piezoelectric actuation of beams *Proc. 30th AIAA/ASME/SAE Structure, Structural Dynamics, and Material Conf. (Washington, DC, April 1989)* pp 2000–10

[9] Lee C K 1990 Theory of laminated piezoelectric plates for the design of distributed sensors/actuators. Part I: governing equations and reciprocal relationships *J. Accoust. Soc. Am.* **87** 1144–58

[10] Lam K Y, Peng X Q, Liu G R and Reddy J N 1997 A finite-element model for piezoelectric composite laminates *Smart Mater. Struct.* **6** 583–91

[11] Lam K Y and Ng T Y 1999 Active control of composite plates with integrated piezoelectric sensors and actuators under various dynamic loading conditions *Smart Mater. Struct.* **8** 223–37

[12] Liu G R, Peng X Q, Lam K Y and Tani J 1999 Vibration control simulation of laminated composite plates with integrated piezoelectrics *J. Sound Vib.* **220** 827–46

[13] Tzou H S and Zhong J P 1993 Electromechanics and vibrations of piezoelectric shell distributed systems *J. Dynam. Syst. Measurements Control* **115** 506–17

[14] Peng X Q, Lam K Y and Liu G R 1998 Active vibration control of composite beams with piezoelectrics: a finite model with third-order theory *J. Sound Vib.* **209** 635–50

[15] Liu G R and Tani J 1994 Surface waves in functionally gradient piezoelectric plates *Trans. ASME J. Vib. Acoust.* **116** 440–8

[16] Pai P F, Nayfe A H, Oh K and Mook D T 1993 A refined nonlinear model of composite plates with integrated piezoelectric actuators and sensors *Int. J. Solids Struct.* **30** 1603–30

[17] Cheng J Q *et al* 2000 Effect of electric fields on the bending behavior of PZT-5H piezoelectric laminates *Smart Mater. Struct.* **9** 824–31

[18] Williams J G 1988 On the calculation of energy release rates for crack laminates *Int. J. Fracture* **36** 101–19

[19] Chaudhuri R A and Kabir Humayun R H 1992 Influence of lamination and boundary constraints on the deformation of moderately thick cross-ply rectangular plates *J. Composite Mater.* **26** 51–77

[20] Chaudhuri R A and Kabir Humayun R H 1993 Sensitivity of the response of moderately thick cross ply doubly-curved panels to lamination and boundary constraint—I: theory *Int. J. Solids Struct.* **30** 263–72

[21] Chaudhuri R A 1989 On boundary-discontinuous double fourier series solution to a system of completely coupled P.D.E.s *Int. J. Eng. Sci.* **27** 1005–22